Article
Beitr. Phys. Atmosph., May 1993, p. 73–87
0005-8173/93/1–2 0073–15 $ 3.00/0
Vol. 66, No.1–2

A Fast Six-Flux Radiative Transfer Method for Application in Finite Cloud Models

by K. M. GIERENS

DLR, Institut für Physik der Atmosphäre, 8031 Oberpfaffenhofen, Germany

(Manuscript received November 30, 1992; accepted March 30, 1993)

Abstract

A six-flux radiative transfer model on a discrete cubic lattice is proposed as a possibility to investigate simultaneously radiation, cloud microphysics, dynamics, and their complex interaction. The present paper concentrates on the treatment of the radiative transfer. An analytical solution is derived and a numerical approximation to this. The cut off error is estimated and an expression for the flux divergence is given. Furthermore, a new fast method is presented for the computation of the multiple scattering operator for a homogeneous cuboid region. The code is tested by calculation of the radiance pattern emerging from a cubic styrofoam cloud model.

Zusammenfassung

Eine schnelle Sechs-Strom Strahlungstransportmethode zur Anwendung in Modellen endlicher Wolken

Es wird vorgeschlagen, zur simultanen Untersuchung von Strahlung, Wolkenphysik und -dynamik, sowie derer komplexen Wechselwirkung ein Sechs-Strom Strahlungstransportmodell zu verwenden, welches auf einem diskreten kubischen Gitter arbeitet. Die Behandlung des Strahlungstransports bildet das Thema des vorliegenden Artikels. Es wird eine analytische Lösung und eine entsprechende numerische Näherung abgeleitet. Der Abbruchfehler wird abgeschätzt und ein Ausdruck für die Flußdivergenz angegeben. Des weiteren wird eine schnelle Methode eingeführt, mit der für ein homogenes würfelförmiges Gebiet der Operator für die Vielfachstreuung bestimmt werden kann. Das Programm wird getestet anhand einer Berechnung des Ausstrahlungsmusters eines würfelförmigen Styropormodells einer Wolke.

1 Introduction

Clouds currently are the most important source of uncertainty for the prognosis of the evolution of the climate. One step toward a better understanding of the role of clouds in climate change is a realistic modeling of the complex interaction of radiative transfer, cloud microphysics, and cloud dynamics. Currently, these aspects are often treated seperately: three-dimensional radiative transfer is studied in clouds which do not evolve in time and, on the other hand, the life cycle of clouds is studied with simplified radiation schemes.

In these latter cases, the heating and cooling rates may be given explicitly as certain functions of the liquid and/or ice water path (parameterization of the radiative transfer, Somieski et al., 1988 investigate some examples), or the transport of radiation is implemented as a two-stream approximation (e.g. Bott et al., 1990; Liou and Zheng, 1984; Starr and Cox, 1985). These, however, cannot describe horizontal radiative interactions within inhomogeneous clouds or between different clouds in a cloud field, which may be important since three-dimensional radiative transfer computations show that a large part of the photons which enter a cloud from top or bottom leave it through the side faces (Welch and Zdunkowski, 1981). Three-dimensional radiative transfer models (Monte Carlo, or analytical approximations, e.g. Davies, 1978) generally need too much computer time. This renders them inappropriate for use in dynamical cloud models (Trautmann and Zdunkowski, 1986). The diffusion approximation (Gube et al., 1980) is only valid in very homogeneous clouds (Lovejoy et al., 1990).

In a recent series on "Discrete Angle (DA) Radiative Transfer" (Lovejoy et al., 1990; Gabriel et al., 1990; Davis et al., 1990) it is pointed out that the optical properties of a medium (e.g. transmission or albedo) are essentially influenced by spatial varia-

bility in the optical density field whereas the angular dependence of the single scattering process is less important. In the modeling of radiative transfer in clouds and cloud fields it is therefore reasonable to concentrate on their spatial variability and it is justified to treat the angular redistribution of photons in the single scattering process in a simplified manner.

In the present paper we propose the DA (3, 6) case (i.e. 3 dimensions, 6 beam directions) as a useful tool for studying clouds and the interaction between radiation, microphysics, and dynamics in an efficient way, i.e. the required computer time is not too large. Since usually hydrodynamical codes work on a spatially discretized grid we will investigate the radiative transfer on a cubic lattice, which is the appropriate geometry for the spatially discretized DA (3, 6) case (see Lovejoy et al., 1990). The radiation is then allowed to flow along straight lines parallel to the {x, y, z} coordinate axes. The scattering (single or multiple) takes place at the regularly arranged grid points and redistributes the photons between the six allowed directions.

The idea of six-flux radiative transfer models is not new. Already 1955 Chu and Churchill developed such a model for a continuous space and plane parallel media. However, whereas we intend to allow for three-dimensional radiative interactions in clouds, their intention was to better represent the continuous scattering phase function than it is possible with two-component approximations. They presented an energy conserving mapping of the continuous phase function onto the discrete one, but pointed out that generally the mapping is not unique and must be justified by a practical point of view. Here we assume the discrete scattering function (matrix) to be given.

It is possible to derive an analytic solution for the present example of radiative transfer (Section 2). Unfortunately, a computer cannot calculate the analytic solution directly since too much memory would be necessary. Instead the true intensity field must be approximated by an iterative procedure (Section 3). However, the analytic solution allows us to determine the accuracy reached after a number of iterations (Section 3.2). The expression for heating and cooling rates (flux divergence) is derived in Section 4. In Section 5 we introduce a new fast method for the computation of the scattering matrix for a whole grid cell from the given phase matrix for the single scattering process. We then describe a test case (radiative transfer through a cubic cloud model made of styrofoam) in Section 6, and conclude in Section 7 by summarizing the results.

2 Analytical Solution

2.1 Preliminaries

In the following we shall use the word "intensity" for the characterization of the radiation field. However, since we are dealing with a six-flux method the meaning of "intensity" is somewhat different to its usual one in continuous radiative transfer. On the one hand, if there is no extinction the intensity stays constant along a ray. This is a fundamental property of the intensity. On the other hand, the discrete angle intensity has "flux-density" like character because the intensity field is a sum of delta functions in solid angle space. Thus, discrete angle intensities can be considered components of flux density vectors (cf. Lovejoy et al., 1990).

The present formulation of radiative transfer is independent of wavelength. The direct solar beam is not separated from the diffuse radiation field. The solar flux density outside the model region is splitted into its cartesian components which in turn are added to the diffuse radiation field incident on the model region. These constitute the boundary conditions for the calculation. We include the thermal emission of each cell in order to allow also the treatment of the infrared spectral region.

We now derive an analytical solution for the determination of the six intensities that emerge from every cell in the grid. It is assumed that the optical properties of the cells are arbitrary, but given. The determination of these is treated in Section 5.

The solution is achieved by iterated application of the interaction principle (Preisendorfer, 1965) by which the intensities (radiances) emerging from a cell are linearly related to those irradiating it from neighbouring ones. Every iteration enlarges the "interaction radius" of a cell by taking into account the next generation of neighbours (i.e. the neighbours' neighbours). The process converges when the interaction radius of each cell comprises the whole lattice.

2.2 The Interaction Principle for a Single Cell

Consider a single cubic cell and its six neighbours (Figure 1). Let the cell be labelled with the three indices (ijk), the neighbours with (i' j' k'). The intensity emerging from cell (ijk) in direction n is I_n (ijk). Internal thermal sources can be written according to Kirchhoff's law as $[1 - \pi\,(ijk)]\,B\,(ijk)$ where $1 - \pi\,(ijk)$ is the probability of absorption in

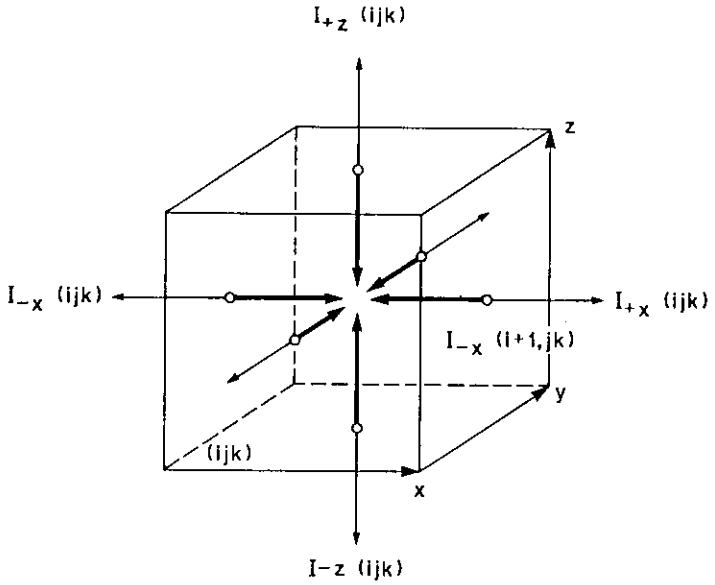

Figure 1 Illustration of the interaction principle for a single cell (ijk): The emergent intensities (thin arrows, e.g. $I_{+x}(ijk)$) depend linearly on the incident intensities (thick arrows, e.g. $I_{-x}(ijk)$)

cell (ijk) and B (ijk) is the Planck function. Then the interaction principle including thermal sources reads:

$$I_n(ijk) = \sum_{m=1}^{6} \sigma_{nm}(ijk)\, I_m[i'(m)\, j'(m)\, k'(m)] + [1-\pi(ijk)]\, B(ijk), \quad n, m \in \{+x, -x, +y, -y, +z, -z\}. \quad (1)$$

Here, σ_{nm} is the probability for scattering of radiation from direction m into direction n and $\pi = \sum_m \sigma_{nm}$ is the total scattering probability in a single cell. It is assumed that the scattering probability depends only on the relative angle between incident and outgoing directions. In this case, for a cubic cell, the 6×6 matrix σ_{nm} is symmetric and contains only three different values: the transmission probability $\sigma_{nn} = T(ijk)$, the reflection probability R (ijk) and the probability for scattering by 90°, S (ijk). Eq. (1) can then be written in more detail (e.g. for the + x direction):

$$\begin{aligned} I_{+x}(ijk) = {} & T(ijk)\, I_{+x}(i-1, jk) + \\ & + R(ijk)\, I_{-x}(i+1, jk) + \\ & + S(ijk)\,[I_{+y}(i, j-1, k) + \\ & + I_{-y}(i, j+1, k) + \\ & + I_{+z}(ij, k-1) + I_{-z}(ij, k+1)] + \\ & + [1-\pi(ijk)]\, B(ijk). \end{aligned} \quad (2)$$

(Figure 1). The interaction principle is valid as long as σ_{nm} is independent of the incident intensities, i.e. in the regime of linear optics, which is always fulfilled in the atmosphere.

2.3 The Interaction Principle for the Whole Grid

Consider an intensity vector $\tilde{I} = (\tilde{I}_0, \tilde{I}')^\dagger$ († means transposition) that consists of the intensities $\tilde{I}'$ for the six directions in all cells and, additionally, the intensities $\tilde{I}_0$ that enter the lattice from outside. The latter are provided as boundary conditions. We must construct then from the single scattering matrices $\sigma_{nm}(ijk)$ a grand matrix $\boldsymbol{\Sigma}$ that contains all scattering probabilities for all cells. Similarly to $\tilde{I}$ we introduce a source vector $(\tilde{0}, \tilde{B})^\dagger$ that comprises the sources $[1-\pi(ijk)]\, B(ijk)$ of all cells ($\tilde{0}$ is the null vector with the same dimension as $\tilde{I}_0$). The interaction principle can then be written for all cells simultaneously:

$$\tilde{I}^{(t+1)} = \boldsymbol{\Sigma}\, \tilde{I}^{(t)} + (\tilde{0}, \tilde{B})^\dagger. \quad (3)$$

This equation can be interpreted as follows: $\tilde{I}^{(t)}$ represents the intensity distribution at "time" t (iteration counter). These intensities are redistributed by scattering (and absorption). This is done by the action of $\boldsymbol{\Sigma}$ which describes the transport of photons from all cells to their immediate neighbours, the absorption, and the transport of photons from outside into the cells at the surface of the lattice and vice versa. In each iteration cycle the internal sources are added to the intensities and redistributed then in the next cycle. In the limit $t \to \infty$ the intensity distribution gets stationary, i.e. the iteration procedure converges. Mathematically, convergence is guaranteed since the row sums of $\boldsymbol{\Sigma}$ are less than or equal to unity. This follows from the physical condition $\pi = T + R + 4S \leq 1$.

The stochastic nature of the scattering process and the probabilistic interpretation of T, R, and S suggests to consider Eq. (3) a stochastic process, where $\tilde{I}^{(t)}$ can be conceived a stochastic state vector and $\boldsymbol{\Sigma}$ a transition operator. Since $\tilde{I}^{(t)}$ depends only on $\tilde{I}^{(t-1)}$ and not on earlier states, Eq. (3) describes a Markov chain. We can therefore use the techniques of probability theory to derive an analytic solution for the DA radiative transfer on a cubic lattice.

2.4 Solution

We order the intensity vector in the following way:

$$\tilde{I} = (\tilde{I}_0, \tilde{I}(1), \tilde{I}(2), \ldots, \tilde{I}(\nu), \ldots, \tilde{I}(\nu_m))^\dagger. \quad (4)$$

$\tilde{I}_0$ is the vector consisting of the boundary values (i.e. the intensities that irradiate the lattice from outside). $\tilde{I}(\nu)$ are the six intensities that emerge from cell ν (we map the index triple (ijk) onto a single one). The number of cells is ν_m. With $\tilde{I}$ organized in this way, $\mathbf{\Sigma}$ obtains the canonical form (Goodman, 1988):

$$\mathbf{\Sigma} = \begin{pmatrix} \mathbf{1} & \mathbf{0} \\ \mathbf{R} & \mathbf{Q} \end{pmatrix}, \tag{5}$$

where $\mathbf{1}$ is the identity matrix, $\mathbf{0}$ the null matrix, and $\mathbf{R}$ and $\mathbf{Q}$ are matrices which contain the scattering probabilities T (ν), R (ν), and S (ν) for all the cells. Let the number of elements of the vector $\tilde{I}_0$ be n and that of $\tilde{I}$ be n + m. Then the dimensions of the blocks of $\mathbf{\Sigma}$ are dim $(\mathbf{1}) = n \times n$, dim $(\mathbf{0}) = n \times m$, dim $(\mathbf{R}) = m \times n$, and dim $(\mathbf{Q}) = m \times m$. Whereas $\mathbf{R}$ describes the scattering of the incident photons in the cells on the surface of the lattice, $\mathbf{Q}$ describes the radiative interaction of every cell with its six neighbours. In order to find the solution vector $\tilde{I}^{(\infty)}$ we must compute $\lim_{t\to\infty} \mathbf{\Sigma}^t$. According to Goodman (1988)

$$\lim_{t\to\infty} \mathbf{\Sigma}^t = \begin{pmatrix} \mathbf{1} & \mathbf{0} \\ \mathbf{NR} & \mathbf{0} \end{pmatrix}, \tag{6}$$

where $\mathbf{N} = (\mathbf{1} - \mathbf{Q})^{-1}$. $(\mathbf{1} - \mathbf{Q}$ is invertible and $\lim_{t\to\infty} \mathbf{Q}^t = \mathbf{0}$ because $\mathbf{Q}$ is substochastic, i.e. $\sum_j Q_{ij} \le 1$; see Goodman, 1988). From this form of the limit matrix we find that an initial internal intensity distribution $[\tilde{I}^{(t=0)}(1, 2, \ldots, \nu_m)]^\dagger$ does not at all affect the solution, since only the null matrix in the solution acts on these intensities. Physically, this follows from the fact that photons initially distributed throughout the lattice will either leave it or be absorbed within a finite time. Only the permanent sources, $\tilde{I}_0$ and $\tilde{B}$ appear in the solution. The only block of $\mathbf{\Sigma}$ that acts on $\tilde{B}$ is $\mathbf{Q}$. In the limit $t \to \infty$ this yields a contribution $(\mathbf{1} - \mathbf{Q})^{-1} \tilde{B} = \mathbf{N}\tilde{B}$. The searched for analytic solution therefore takes on the compact form:

$$\tilde{I}^{(\infty)} = \begin{pmatrix} \mathbf{1} & \mathbf{0} \\ \mathbf{NR} & \mathbf{N} \end{pmatrix} \begin{pmatrix} \tilde{I}_0 \\ \tilde{B} \end{pmatrix}. \tag{7}$$

3 Numerical Solution

3.1 Numerical Approximation

The analytical solution of the discrete angle radiative transfer problem on a cubic lattice is merely of theoretical interest because for nearly all applications the matrix $\mathbf{N}$ is by far too large to be hold in a computer memory. Although $\mathbf{Q}$ is sparse, $\mathbf{N}$ will be full since, as we saw, through its action information is transmitted from every cell to every other cell in the grid.

For a numerical approximation we must therefore go back to Eq. (3). We rewrite it now in the following form:

$$\tilde{I}'^{(t+1)} = \mathbf{R}\tilde{I}_0 + \mathbf{Q}\tilde{I}'^{(t)} + \tilde{B} =: \mathbf{Q}\tilde{I}'^{(t)} + \tilde{k}, \tag{8}$$

where $\tilde{I}'^{(t)} = [\tilde{I}^{(t)}(1), \ldots, \tilde{I}^{(t)}(\nu), \ldots, \tilde{I}^{(t)}(\nu_m)]^\dagger$ (i.e. the background intensities have been separated from $\tilde{I}$). The permanent photon sources $\mathbf{R}\tilde{I}_0$ and $\tilde{B}$ have been comprised in the constant vector $\tilde{k}$. (In the following we shall leave out the prime from $\tilde{I}'$). Eq. (8) is now iterated numerically until a certain convergence criterion (see below) is fulfilled. Here we can exploit the sparseness of $\mathbf{Q}$ in that only its nonzero elements are to be hold in the computer memory. Iterative equations like that above are well known from the numerical treatment of elliptic differential equations (cf. Varga, 1962).

For the considerations in the next Section it will prove useful to have the limit vector $\tilde{I}^{(\infty)}$ in the form:

$$\tilde{I}^{(\infty)} = \mathbf{N}\tilde{k} = (\mathbf{1} - \mathbf{Q})^{-1}\tilde{k}. \tag{9}$$

3.2 Convergence and Relative Error

Let us define the relative error δ of the iteration scheme as follows:

$$\delta(t) := \frac{\|\tilde{I}^{(\infty)} - \tilde{I}^{(t)}\|}{\|\tilde{I}^{(\infty)}\|}, \tag{10}$$

where $\|\cdot\|$ designates a vector norm of arbitrary degree. It is shown in various textbooks on numerical methods (e.g. Varga, 1962) that

$$\delta(t) \le \|\mathbf{Q}^t\| \cdot \delta(0), \tag{11}$$

where, $\|\cdot\|$ is the natural matrix norm induced by the former vector norm. Generally, convergence is achieved the faster the smaller the row sums of $\mathbf{Q}$ (i.e. $\sum_j Q_{ij}$). Physically, this means that absorption enhances the convergence speed whereas a high albedo everywhere makes more iterations necessary. This can be understood as follows: Absorption restricts the interaction region of a cell. Thus a few applications of the transfer matrix $\mathbf{Q}$ suffice to

establish a mutual correspondence between the cells in the restricted interaction region. Conservative scattering, on the other hand, couples all cells to each other. Thus the interaction region of every cell is the whole lattice. Then many iterations are required to transfer the photons via (infinitely) many possible paths from any cell to any other.

Whereas the inequality above is useful for theoretical considerations about the convergence behaviour, it is impracticable for the control of the convergence at run time of the program since $\delta(0)$ is unknown implicitely. Instead we are seeking for a criterion that involves the current estimate of the intensity vector and that is easy and fast to compute. Such a criterion can be derived from the following inequality:

$$\begin{aligned}\delta(t) &= \frac{||\tilde{I}^{(\infty)} - \tilde{I}^{(t)}||}{||\tilde{I}^{(\infty)}||} = \\ &= \frac{||(\mathbf{1}-\mathbf{Q})^{-1}(\tilde{I}^{(t+1)} - \tilde{I}^{(t)})||}{||(\mathbf{1}-\mathbf{Q})^{-1}\tilde{k}||} \\ &\le \frac{||(\mathbf{1}-\mathbf{Q})^{-1}||\,||\tilde{I}^{(t+1)} - \tilde{I}^{(t)}||}{||\tilde{k}||}\end{aligned} \tag{12}$$

since $||(\mathbf{1}-\mathbf{Q})^{-1}\tilde{k}|| \ge ||\tilde{k}||$. The term $||(\mathbf{1}-\mathbf{Q})^{-1}||$ in the nominator needs too much time to be computed numerically and must be replaced by a majorant that is easy to calculate. For this purpose we use the triangle inequality:

$$\begin{aligned}||(\mathbf{1}-\mathbf{Q})^{-1}|| &= ||\mathbf{1}+\mathbf{Q}+\mathbf{Q}^2+\mathbf{Q}^3+\ldots|| \\ &\le 1 + ||\mathbf{Q}|| + ||\mathbf{Q}^2|| + ||\mathbf{Q}^3|| + \ldots\end{aligned} \tag{13}$$

Let p be the first index for which $||\mathbf{Q}^p|| < 1$, i.e. for any index $t < p$, $||\mathbf{Q}^t|| = 1$. Physically, p is the minimum distance (in unit of grid cells) from any cell to the surface of the lattice (if scattering is conservative; otherwise it is the shortest distance from any cell to any absorbing cell or to the surface):

$$p \le \text{int}\,[(1/2)\min(i_{max}, j_{max}, k_{max}) + (1/2)] \tag{14}$$

Let us write "ρ" for $||\mathbf{Q}^p||$. Then $||\mathbf{Q}^t|| \le \rho$ for $t \ge p$ and $||\mathbf{Q}^{np}|| \le \rho^n$. Thus

$$\begin{aligned}&1 + ||\mathbf{Q}|| + ||\mathbf{Q}^2|| + ||\mathbf{Q}^3|| + \ldots \\ &\le p + p\rho + p\rho^2 + p\rho^3 + \ldots = p/(1-\rho)\,.\end{aligned} \tag{15}$$

The desired convergence criterion is therefore:

$$\delta(t) \le \frac{p}{1-\rho}\,\frac{||\tilde{I}^{(t+1)} - \tilde{I}^{(t)}||}{||\tilde{k}||} \le \varepsilon\,, \tag{16}$$

where ε is a prescribed accuracy.

The question arises whether it is possible to enhance the rate of convergence by overrelaxation. This is indeed the case when the intensity distribution is to be computed once for a medium with fixed properties. However, in the context of dynamical cloud models overrelaxation is not always a good choice. In this case the intensity field must be computed, say, every ten minutes. When the atmosphere has not changed too much in this time, the new intensity vector will not be too different from the old one. Thus many iterations can be saved if the calculation starts with the old intensity vector instead of $\tilde{I}^{(t=0)} = 0$. But then it cannot be guaranteed in the first p iterations that the new solution vector is approached in a monotonic way. This is a purely physical effect that originates from the inhomogeneity of the medium. If the solution is approached in a non monotonic way overrelaxation deteriorates the convergence.

4 Flux Divergence and Heating Rate

Consider two adjacent cells in the x-direction (Figure 2). The net flux in the + x-direction through the boundary of the two cells is:

$$F_x(ijk) = I_{+x}(ijk) - I_{-x}(i+1, jk)\,. \tag{17}$$

(cf. the introductory remarks about the meaning of "intensity" in the discrete angle case in Section 2.1). The corresponding expressions for the y and z-directions are similar. We can compute the divergence of the flux vector $\mathbf{F} = (F_x, F_y, F_z)^\dagger$ using Gauss' theorem:

$$\int \mathbf{F}(ijk)\cdot d\mathbf{A}(ijk) = \int \nabla\cdot\mathbf{F}\,dV(ijk) \approx \nabla\cdot\mathbf{F}\,l^3. \tag{18}$$

Here, $d\mathbf{A}(ijk)$ is a surface element of cell (ijk), $dV(ijk)$ is a corresponding volume element. The

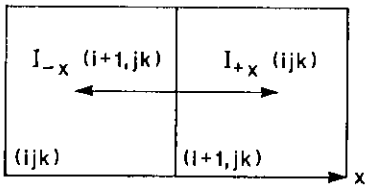

Figure 2 Illustration for the flux calculation.

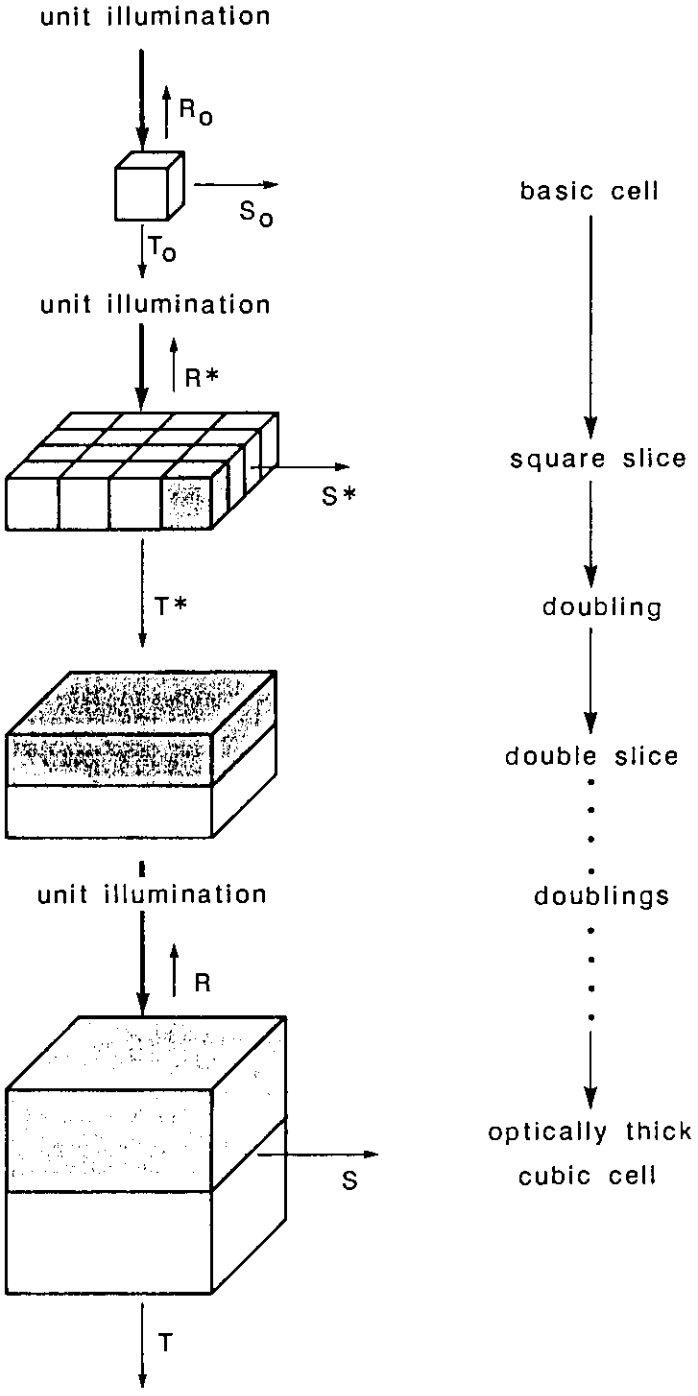

Figure 3 Illustration of the slice doubling method.

volume of the cell is l^3. Evaluation of the surface integral yields:

$$\begin{aligned}\nabla \cdot \mathbf{F} l^3 \approx\ & [F_x(ijk) - F_x(i-1, j\,k)] \cdot l^2 \\ & + \text{corresponding expressions for y and z} \\ =\ & [I_{+x}(ijk) - I_{-x}(i+1, j\,k) - I_{+x}(i-1, j\,k) \\ & + I_{-x}(ijk)] \cdot l^2 \\ & + \ldots \end{aligned} \tag{19}$$

We now use the interaction principle (Eqs. (1) and (2)) again in order to express the intensities emerging from cell (ijk) in terms of the incident intensities. Furthermore, we introduce the mean of intensities incident on cell (ijk):

$$\begin{aligned} J(ijk) := \frac{1}{6} & [I_{+x}(i-1, j\,k) + I_{-x}(i+1, j\,k) + \\ & + I_{+y}(i, j-1, k) + I_{-y}(i, j+1, k) + \\ & + I_{+z}(i\,j, k-1) + I_{-z}(i\,j, k+1)] . \end{aligned} \tag{20}$$

We can then write the flux divergence in a concise form as:

$$\nabla \cdot \mathbf{F} = (6/l)\,[1 - \pi(ijk)]\,[B(ijk) - J(ijk)] . \tag{21}$$

The corresponding heating (or cooling) rate is $c_p \rho\, \partial T/\partial t = -\nabla \cdot \mathbf{F}$. Eq. (21) is easy to interprete in physical terms: $1 - \pi$ is the probability of absorption in cell ijk. The heating rate is proportional to this, since only the absorbed photons feed energy into the cell. Further, the heating rate is proportional to J – B, which in turn is proportional to the difference of the numbers of photons entering cell ijk from outside (heating) and the number of photons created inside the cell and leaving it (cooling).

5 The Scattering Matrix for a Single Cell

5.1 Multiple Scattering and Three-Dimensional Doubling

In this Section we propose an efficient method for computation of the matrix $\sigma = (\sigma_{nm})$ which describes the transfer properties T (transmission), R (reflection) and S (scattering by an angle of 90 degrees) of a single cell. This matrix, as will be recognized lateron, is a complicated function of the elements of the single scattering matrix **P** which is assumed to be known for the ice particle and water drop mixture in the cell. According to the discussion in Lovejoy et al., (1990), the two matrices share the same structure:

$$\sigma = \begin{pmatrix} T & R & S & S & S & S \\ R & T & S & S & S & S \\ S & S & T & R & S & S \\ S & S & R & T & S & S \\ S & S & S & S & T & R \\ S & S & S & S & R & T \end{pmatrix}, \quad \mathbf{P} = \begin{pmatrix} t & r & s & s & s & s \\ r & t & s & s & s & s \\ s & s & t & r & s & s \\ s & s & r & t & s & s \\ s & s & s & s & t & r \\ s & s & s & s & r & t \end{pmatrix} .$$

Here we have made two assumptions: first, the phase function should depend only on the relative scattering angle (i.e. ice needles with a preference for a certain orientation in space cannot be treated); second, the cells must be cubic. These two assump-

tions allow the two matrices to be completely determined by only three different quantities, namely {t, r, s} and {T, R, S}, respectively.

The relation between σ and $\mathbf{P}$ depends on the optical depth τ through the cell. Let us first consider the case of an optically thin cell (i.e. $\tau \ll 1$). In this case the optical depth can be interpreted as the probability for a photon travelling through the cell to suffer a single interaction with the material inside. In such an event the photon has the possibilities either to change its direction (by 0, 90, or 180 degree) or to be absorbed, with the corresponding probabilities t, s, r and $a = 1 - t - 4s - r$. The probabilities for the joint events "single interaction and change of direction by a certain angle (or absorption)" are given by the product rule (e.g. $\tau \cdot s$) since the two parts of these joint events are independent. A negligible fraction $\mathcal{O}(\tau^2)$ of the photons will interact twice or more, and a fraction $1 - \tau$ will not interact at all. Of course, the noninteracting photons are transmitted. Thus the probabilities for transmission, reflection and scattering by 90° for an optically thin cubic cell are:

$$\begin{aligned} T &= (1-\tau) + t \cdot \tau + \mathcal{O}(\tau^2) \\ R &= r \cdot \tau + \mathcal{O}(\tau^2) \\ S &= s \cdot \tau + \mathcal{O}(\tau^2) \end{aligned} \tag{22}$$

or, in compact notation (Lovejoy et al., 1990):

$$\sigma = \mathbf{1} - (\mathbf{1} - \mathbf{P})\,\tau + \mathcal{O}(\tau^2)\,. \tag{23}$$

If the cell is optically thicker ($\tau \approx 1$ or $\tau > 1$) more and more photons interact twice or more with the matter in the cell. The term $\mathcal{O}(\tau^2)$ is then no longer negligible, hence Eqs. (22) and (23) must not be used in this case.

A natural strategy for optically thick cells is to partition them into a number of optically thin cubic subcells. We will call such a unit a basic cell. For these, Eqs. (22) and (23) are valid. In principle, the scattering matrix σ for the cell can be computed from that of the basic cell, σ_0, by application of the method given in the foregoing Sections or by any other exact method, e.g. Monte Carlo. However, these methods, if applied to every single cell, consume too much computer time. This renders them inappropriate for implementation in models of the atmosphere.

A fast and elegant method that is apt for a six flux-model is the three dimensional doubling method proposed by Cogley (1981). This procedure starts from a basic cell (optical depth τ_0) which is then doubled stepwise in the x, y, and z direction (see Figure 2 in Cogley, 1981). The configuration is irradiated from the top with unit intensity (– z direction). The three doubling steps lead to a new cubic cell with optical depth $2\,\tau_0$. The procedure is iterated until finally the optical depth $\tau = 2^n\,\tau_0$ of the original optically thick cell is reached.

Gabriel et al. (1990) already recognized that the three dimensional doubling method is not exact (even within the context of a six-flux model). This can be explained as follows: After the first two doubling steps we have a square disk consisting of four identical basic cells. It is essential for the doubling formulae to hold that these four cells are located at equivalent places (otherwise more than one e.g. transmission probability would be necessary). However, in the next doubling cycle three of the four original basic cells get new neighbours in the x and y dimension, i.e. the four basic cells are no longer at equivalent places, which means that this premise is violated in each further cycle except the first one. From this it follows that the x and y doubling steps produce errors in each iteration. The doubling steps in the z dimension, however, do not lead to an error, since these do not abolish the symmetrical order in the x and y dimension. (The z-dimension is distinguished by the test radiation flowing along the z-axis.)

A comparison of the results of the 3-dimensional doubling method with those of Monte Carlo computations (Davis, 1978, see Figure 4) demonstrates that the error introduced by the doubling method is systematic: Whereas the reflection probability R is underestimated, the probability for scattering by 90°, S, comes out too large. The following argument makes this plausible: Consider the radiation when it enters the top face of the cubic cell. In 3-dimensional doubling this face consists of four subcells which are also located at the side faces of this cell. Thus, for the test photons the path out of the side faces of the cell is very short and, consequently, the probability for scattering through the sides of the cell is relatively high. Obviously, this probability is diminished and the backscattering probability grows when the cell is resolved into a larger number of subcells because then only a fraction of these are located at the side faces of the cell and the number of scattering centres in the top face of the cell is enlarged. Consider the extreme case of basic cells with $R_0 = 0$ and $S_0 \neq 0$; as soon as two or more of these basic cells are joined together backscattering becomes possible, thus $R > 0$ although $R_0 = 0$. For this reason Gabriel et al. (1990) directly compute the transfer properties of $4 \times 4 \times 4$ up to $16 \times 16 \times 16$ subcells and iterate this procedure (quadrupling, octupling, ...). This however requires time consum-

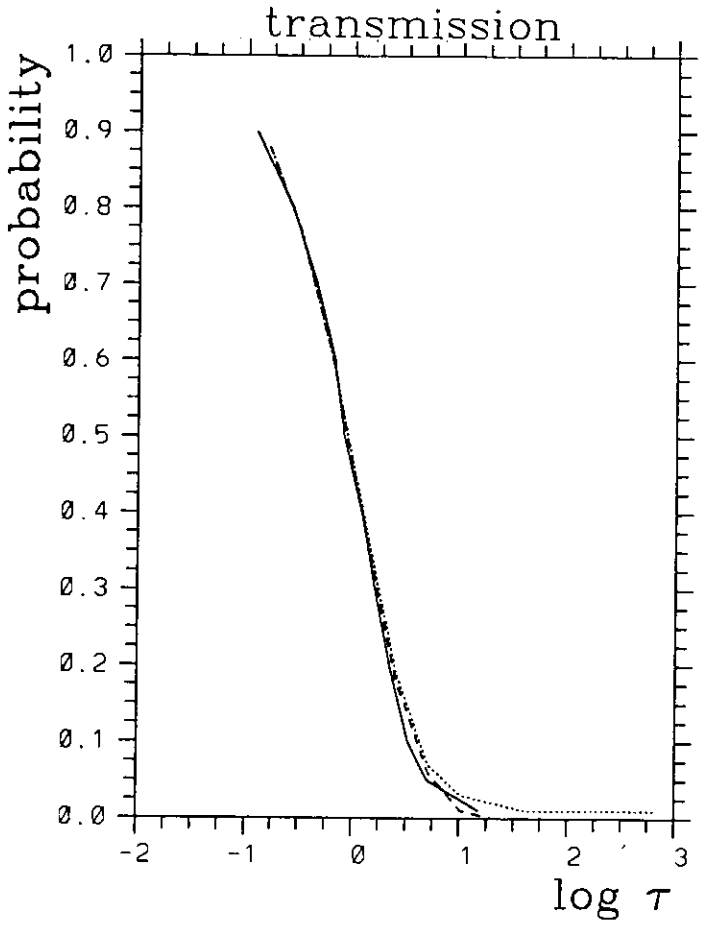

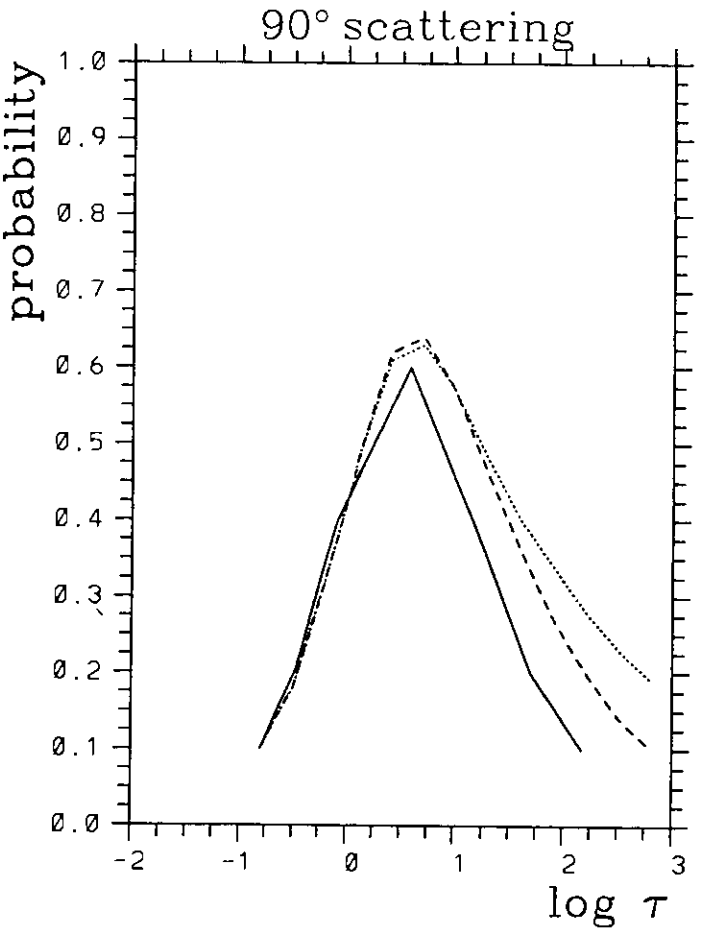

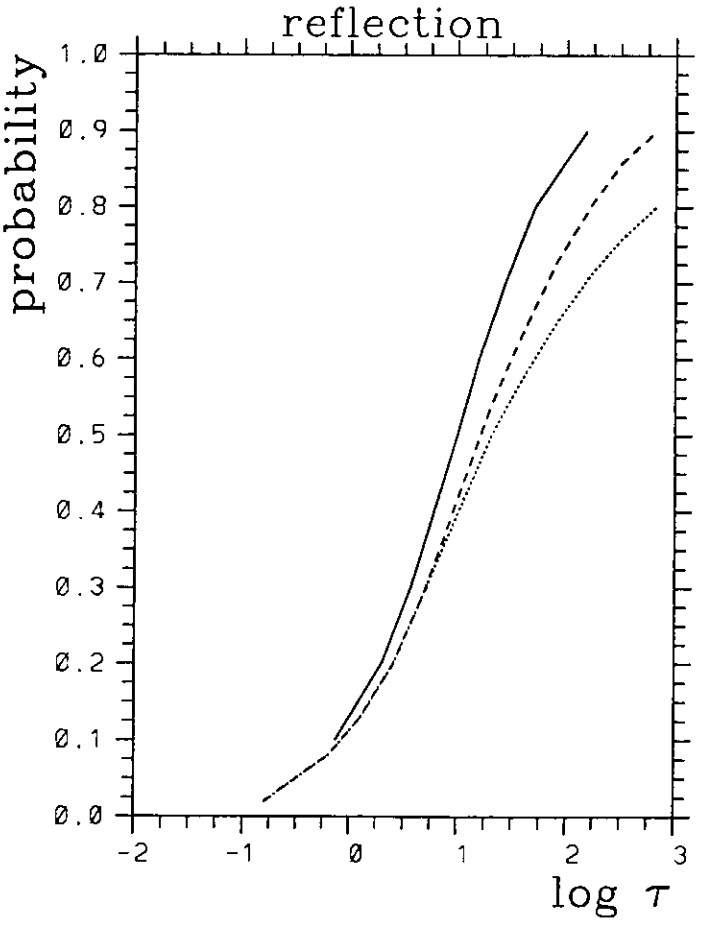

Figure 4 Probabilities for transmission, reflection, and scattering by 90°, as functions of optical depth for cubic clouds with conservative isotropic scattering computed with Monte Carlo (Davies 1978, solid curves), Cogley's three dimensional doubling (dotted), and slice doubling (dashed) methods.

ing numerical solution of the radiative transfer in these $4 \times 4 \times 4$ (and higher) lattices.

5.2 The Slice Doubling Method

We have developed an alternative method that is even faster than 3-dimensional doubling and produces also smaller systematic errors. We call it the slice doubling method. It proceeds as follows (see Figure 3): Starting from a basic cell (τ_0) we calculate the transmission (T*), reflection (R*) and 90° scattering (S*) probabilities for a square plate consisting of $2^n \times 2^n$ basic cells. The plate is irradiated from one of the broad faces with unit intensity. This plate is considered a thin slice of the original optically thick cell. In this configuration only 4 $(2^n - 1)$ out of the 2^{2n} basic cells are located at the side faces of the slice. Thus the error generated in Cogley's method is avoided. The relation between the scattering probabilities for the basic cell, $\{T_0, R_0, S_0, A_0\}$ $(A_0 = 1 - T_0 - R_0 - 4\,S_0)$,

and {T*, R*, S*, A*} is simple:

$$T^* = T_0 + S_0\,\mathscr{C}(\tau) \quad (24)$$

$$R^* = R_0 + S_0\,\mathscr{C}(\tau) \quad (25)$$

$$A^* = A_0 + A_0\,\mathscr{C}(\tau) \quad (26)$$

$$S^* = S_0 - (1/4)\,(2\,S_0 + A_0)\,\mathscr{C}(\tau)\,. \quad (27)$$

These relations can be explained as follows: A photon can be transmitted either directly with probability T_0 or after a random walk through the slice which is taken into account by the correction function $\mathscr{C}(\tau)$. The last step in the random walk (not included in the definition of $\mathscr{C}(\tau)$) is scattering out of the plane of the slice. Similarly, a photon is reflected either directly (R_0) or after a random walk with the last step being a scattering event. In the case of absorption the last step of the random walk is absorption instead of scattering; also the photon can be absorbed directly with probability A_0. Eq. (27) is then a consequence of energy conservation. Since the random walk is initiated by a scattering event, $\mathscr{C}$ is to first order proportional to S_0. Further properties of $\mathscr{C}(\tau)$ are:

(i) $\mathscr{C}(\tau_0) = 0$
(ii) $\mathscr{C}(2\,\tau_0) = 2\,S_0 / (1 - R_0 - S_0)$
(iii) $\mathscr{C}(\tau)$ is strictly monotonically increasing
(iv) $\lim_{t\to\infty} \mathscr{C}(t) = 4\,S_0 / (2\,S_0 + A_0)$.

(i) is trivial, (ii) and (iii) are explained in Appendix A, and (iv) is again a consequence of energy conservation. It follows from Eq. (27) and the postulate $S^* \to 0$ for a horizontally infinite plate.

Unfortunately, the a priori knowledge about the correction function does not suffice to derive $\mathscr{C}(\tau)$ uniquely and exactly. In fact, since the number of possible photon paths increases to astronomical orders of magnitude even for small numbers of basic cells in the slice, the direct calculation of $\mathscr{C}(\tau)$ is unfeasible. Numerical methods consume too much computing time.

Instead we will present a stochastic ansatz that leads to an analytic approximation to $\mathscr{C}(\tau)$. To this end, we treat all 2^{2n} basic cells as equivalent, i.e. we ascribe mean properties of the slice to each basic cell, e.g. the mean distance to the edge, independently of their actual location. With this ansatz, we are now going to compute the probability A* for absorption in the slice. This suffices for the determination of the correction function.

Consider a photon that hits a certain (arbitrary) basic cell. Then there are the following possibilities: (1) direct absorption with probability A_0, (2) scattering into the plane of the slice with probability $4\,\beta\,S_0$. Here, $\beta = 1 - \tau_0/\tau$ corrects for the cells at the edge of the slice, having less than four neighbours (Appendix B). After the first scattering there are the following possibilities for the further fate of the photon in the slice: it can be (3) absorbed (prob. A_0), or (4) change direction with probability $2\,\gamma\,S_0 + R_0$, where $\gamma = 1 - (4/3)\,(\tau_0/\tau) + (2/3)\,(\tau_0/\tau)^2$ (Appendix B). (3) and (4) can take place immediately after (2) or after one, two, three, ..., transmissions. The sum of the probabilities for series of 0, 1, 2, 3, ... transmissions is (Appendix B):

$$\alpha = \frac{1}{1-T_0}\left[1 - \frac{\tau_0}{\tau}\,\frac{2\,T_0 - T_0^2 - T_0^{(\tau/\tau_0)}}{1-T_0}\right]. \quad (28)$$

The factor in brackets corrects for the finite extent of the slice; an infinitely extended slice has $\alpha = 1/(1 - T_0)$. After a change of direction (4) a new series of transmissions starts which ends again with an absorption or a new change of direction, and so forth ad infinitum. This leads to the following expression for A*:

$$\begin{aligned} A^*(\tau) &\approx A_0 + 4\beta S_0\{\alpha\,[A_0 + (2\gamma\,S_0 + R_0) \\ &\quad \times \{\alpha\,[A_0 + (2\gamma\,S_0 + R_0) \\ &\quad \times \{\alpha\,[A_0 + (2\gamma\,S_0 + R_0) \ldots \\ &= A_0 + A_0\,\frac{4\beta S_0 \alpha}{1 - \alpha\,(2\gamma\,S_0 + R_0)}, \end{aligned} \quad (29)$$

from which we get the desired result:

$$\mathscr{C}(\tau) \approx \frac{4\beta S_0 \alpha}{1 - \alpha\,(2\gamma\,S_0 + R_0)}. \quad (30)$$

This approximation of $\mathscr{C}(\tau)$ fulfills the requirements (i)–(iv) for the correction function. The expression is only approximate because in the derivation we do not distinguish between the different basic cells contained in the slice, although they are placed more or less far away from the slice's edge. Instead we treat each basic cell as located in an average environment. The error introduced here is, however, smaller than that generated in the 3-dimensional doubling method. In Figure 4 we compare both methods with exact results of Davis' (1978) Monte Carlo calculations. The comparison has been done for cubic clouds and isotropic conservative scattering. It can be seen that the transmission probability can be computed with great accuracy by both

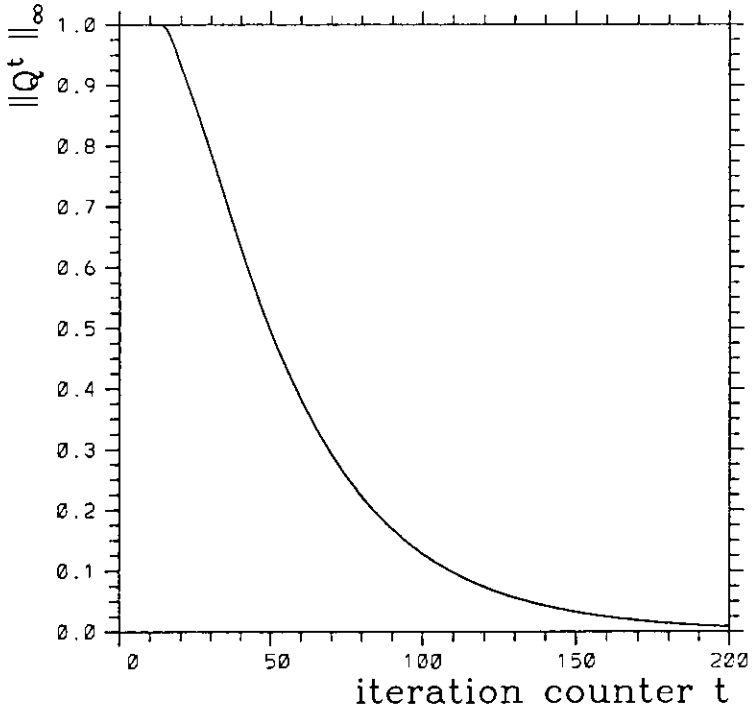

Figure 5 Evolution of the relative error estimate $\| \mathbf{Q}^t \|_\infty$ as a function of the iteration counter t in the test case of Section 6.

Cogley's method and the slice doubling method. At optical depths $\tau > 1$ both methods generally underestimate the reflection probability whereas the scattering probability is overestimated. It is seen that the errors in the slice doubling method are about half those from the 3-dimensional doubling method.

Finally, the calculation of the scattering matrix σ is completed by n-fold application of the doubling formulae on T*, R*, and S*. These are given here for the sake of completeness:

$$\begin{aligned} T(2\tau) &= T(\tau)^2 / [1 - R(\tau)^2] \\ R(2\tau) &= R(\tau) + T(\tau)^2 R(\tau) / [1 - R(\tau)^2] \\ S(2\tau) &= S(\tau) + T(\tau) S(\tau) / [1 - R(\tau)] . \end{aligned} \quad (31)$$

As noted above, these doublings in the direction of the incident unit radiation do not produce any errors.

6 A Test Case

In laboratory simulations of cloud radiances cloud models of styrofoam are illuminated by a lamp, and the radiance pattern exiting the cloud model is then measured. Such an experiment has been performed by Davis and Cox (1986), who used a cubic cloud model with optical depth of 60 along a side. The model was illuminated homogeneously from above through a square aperture with a zenith angle of 0°. The radiance pattern exiting the side of the styrofoam cube was measured and compared to the results of a corresponding Monte Carlo calculation.

We have recalculated the same situation with our model. The cube with $\tau_{tot} = 60$ has been divided into 30^3 cubic cells, each of which had an optical depth $\tau = 2$. We used an Henyey-Greenstein phase function $p_{HG}(\mu) = (1/2)(1 - g^2)(1 + g^2 - 2g\mu)^{-3/2}$ with asymmetry parameter $g = 0.86$ (μ is the cosine of the scattering angle). This is an adequate analytical approximation to the C.1 phase function (Deirmendjian, 1969) at a wavelength of $\lambda = 0.55$ µm used by Davis and Cox (1986) for their calculation. Unfortunately, the mapping of a continuous phase function onto a discrete one is to some degree arbitrary (cf. Chu and Churchill, 1955). Furthermore, since these two probability distributions are essentially different, their moments are not identical. Here we choose a transformation that leaves the first moment ($\langle \mu \rangle = g$) invariant and yields correct values for t, r, and s in the limiting cases of isotropic scattering ($g = 0$) and $g = \pm 1$:

$$\begin{aligned} t &= (1 + g^{1/4} + 3g + g^2) / 6 \\ r &= t - g \\ s &= (1 - t - r) / 4 . \end{aligned} \quad (32)$$

The second moment differs slightly: $\langle \mu^2 \rangle = t + r = (1 + g^{1/4} + g^2)/3$ in the DA case, yet it is $(2 + g^2)/3$ for the Henyey-Greenstein function. This difference is, however, small when the scattering is preferentially forward ($g \lesssim 1$), as it is the case for scattering at cloud particles. The above transformation yields the following single scattering probabilities: $t = 0.88$, $r = 0.02$, $s = 0.025$. The scattering matrix for a cell has been computed using the slice doubling technique with a basic cell of optical depth $\tau_0 = 0.00625$. The result is: $T = 0.791$, $R = 0.036$, $S = 0.043$. Then we have used the discrete angle radiative transfer program to compute the intensity field within the model cloud and emerging from it. After 193 iterations the relative error $\| \mathbf{Q}^{193} \|_\infty$ was less then one percent. This means that the elements in the approximate solution vector $\tilde{I}^{(193)}$ do not differ from the corresponding elements in the exact solution vector $\tilde{I}^{(\infty)}$ by more than one percent. In Figure 5 we demonstrate how convergence is achieved in this case by plotting $\| \mathbf{Q}^t \|_\infty$ against the iteration counter t.

The radiance patterns emerging from different cloud faces are shown in Figures 6, 7, 8. Those from

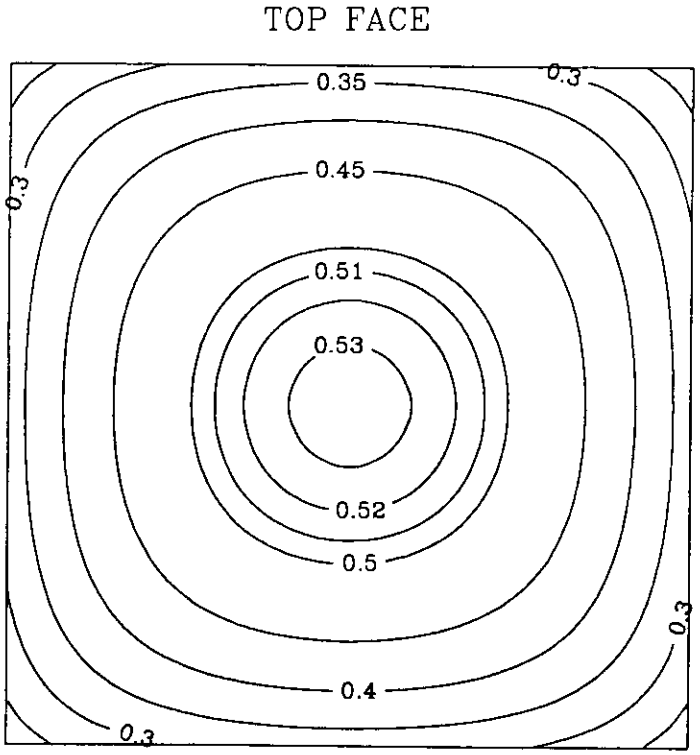

Figure 6 Isophotes of the radiation emergent from the top face of a cubic styrofoam cloud model. The cube is illuminated homogeneously from the top with parallel radiation of unit intensity coming from a lamp at zenith angle 0°. The optical depth of the cube is 60. The scattering is conservative. 41 % of the incident radiation emerges from the top face. The maximum and minimum intensities are $I_{max} = 0.534$ and $I_{min} = 0.214$.

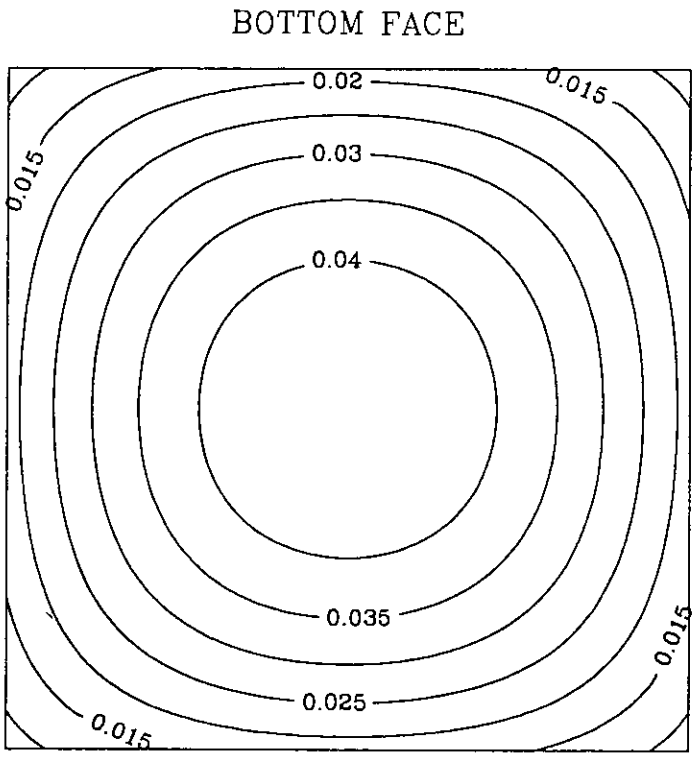

Figure 7 As Figure 6, but for the bottom face of the cube. 3 % of the incident radiation is transmitted through the bottom face. $I_{max} = 0.044$ and $I_{min} = 0.008$.

the top and bottom faces are symmetric around the faces' centres as expected. Since the optical depth is rather large ($\tau_{tot} = 60$), only 3 percent of the incident illumination emerge from the bottom face. The top face, on the other hand, reflects 41 percent of the incoming radiation. The remaining part shines through the sides of the cube (14 percent each).

The radiance pattern from the side faces can be directly compared to those measured and computed by Davies and Cox. Generally, our isophotes match their measured ones very well. However, the isophotes of Davis and Cox show spurious kinks that are presumably an artifact of the plotting routine. Our isophotes are smooth and hence resemble more the impression one has directly from the photograph (Figure 1 in Davis and Cox). The minimum and maximum intensities calculated with the present method match very closely the measured ones, even closer than the corresponding results from the Monte Carlo calculation (see Table 1). The whole computation took only 4 sec CPU time of a single processor of a Cray-YMP.

We have also tested the case of an obliquely illuminated cube. Again a Henyey-Greenstein phase

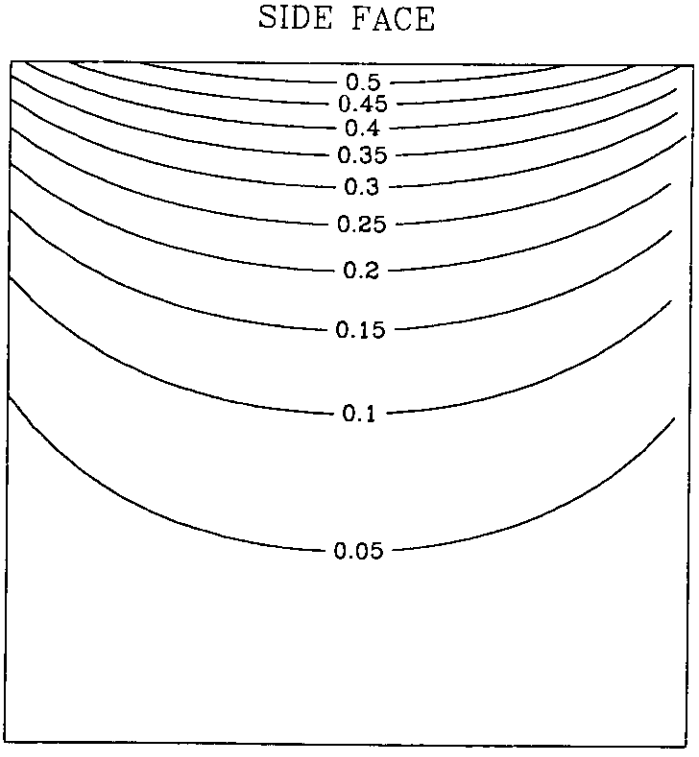

Figure 8 As Figure 6, but for a side face of the cube. Each side contributes 14 % to the emergent radiation, hence totally 52 % of the incident radiation leaves the model cloud via its sides. $I_{max} = 0.549$ and $I_{min} = 0.005$.

function with $\pi_0 = 1$ and $g = 0.86$ was used. We considered cubes with various optical depths, $\tau_{tot} \in \{2, 5, 10, 20, 50, 100\}$. The unit irradiance was supposed to shine on the top face with an zenith angle of 60° and on one side face. The oblique incident unit flux vector was decomposed into two cartesian components, $\mathbf{F}_0 = -\mathbf{i} \sin 60° - \mathbf{k} \cos 60°$ ($\mathbf{i}$, $\mathbf{k}$ are unit vectors in x and z direction). These are the boundary conditions for the problem. The results have been compared with those of the Monte Carlo calculations of Davies (1978, his Figure 6). In Table 2 we list the fraction of incident radiation shining out from different faces of the cube. Generally, the results agree very well with Davies', which shows that for simple cases the DA method is able also to treat incident radiation that does not flow parallel to one of the coordinate axes. In Table 2 we list also the CPU time needed for each case (single processor Cray-YMP).

7 Conclusions

We have developed a 6-flux radiative transfer model which can easily be incorporated into mesoscale atmosphere models. The model is based on the discrete angle approximation that has recently been extensively studied by Lovejoy et al. (1990). We have derived an analytic solution for the DA (3,6) case on a discrete space. This allows to quantitatively determine an upper limit to the relative error in the numerical approximation.

We have furthermore developed a fast method for the computation of scattering probabilities for homogeneous clouds of cuboid shape (the single scattering phase function is assumed to be given). The new technique is faster than Cogley's (1981) three dimensional doubling method and produces smaller errors.

We have tested the model with a calculation of the intensity pattern emergent from an optically thick ($\tau = 60$) cubic styrofoam model of a cloud. The results closely match those measured and computed (Monte Carlo) by Davis and Cox (1986). We have also tested the ability of the model to treat oblique illumination (i.e. incident flux vector not parallel to a coordinate axis). We found that for the simple case of single cubic clouds the results of the DA model agree well with those of the Monte Carlo calculations of Davies (1978). However, if the cloud has a more complicated shape (in particular concave parts with mutual shadowing) or for cloud fields with partial mutual shadowing, it is currently not justified to use our 6-flux model, since then the decomposition of the oblique incident flux into cartesian components leads to an illumination pattern on the clouds that is very different from that produced by the oblique beams themselves.

The radiative transfer model is formulated independent of wavelength in the present paper. Thus its application to monochromatic situations like the experiment with the styrofoam cube is straightforward. However, the treatment of real clouds requires to take into account the whole visual and infrared wavelength region. There are essentially two ways of doing this for the absorption properties of single air molecules: they can be obtained from band models and k-distribution models. The optical properties of ice particles and water drops can be obtained from parameterizations that are based e.g. on Mie calculations (Rockel et al., 1991). Such calculations are, however, beyond the scope of the present paper.

The optical properties of cloud particles and air molecules together with their spatial distribution determine the optical depth of each grid cell. The single cell is assumed to be optically homogeneous, but the optical depth and composition can vary from

Table 1 Measured and computed minimum and maximum intensities emerging from the side of a cubic styrofoam cloud model which is irradiated from above with unit intensity. The experiment and Monte Carlo calculation were performed by Davis and Cox (1986), DA (3,6) refers to the 6-flux model proposed in the present paper.

	experiment	Monte Carlo	DA (3,6)
$\tilde{I}_{min}$	0.006	0.020	0.005
$\tilde{I}_{max}$	0.540	0.520	0.549

Table 2 Fraction of incident flux shining through different faces of cubic clouds. The zenith angle of the incident flux is 60 degree. A Henyey-Greenstein phase function with $\pi_0 = 1$ and $g = 0.86$ is used. MC refers to Monte Carlo calculations of Davies (1978), DA refers to the 6-flux model proposed in the present paper.

	top		bottom		4 sides		CPU
τ_{tot}	MC	DA	MC	DA	MC	DA	sec.
2	.02	.04	.34	.32	.64	.64	2.1
5	.06	.08	.30	.26	.64	.66	2.2
10	.11	.13	.25	.21	.64	.66	2.5
20	.18	.18	.20	.16	.62	.66	2.8
50	.25	.23	.13	.11	.62	.66	3.9
100	.30	.27	.08	.08	.62	.65	5.9

cell to cell, hence the transfer characteristics of the single cells can be different. They can be computed with Eq. (23) for optically thin cells or by means of the slice doubling method, if a cell is optically thick. When this preparation work is done, the radiative transfer through the whole inhomogeneous cloud can be computed with the method described in Section 3.

In models of the atmosphere, the radiative transfer has to be computed from time to time after a number of dynamical time steps. In the first instance, when the calculation begins with $\tilde{I}_0 = 0$, the number of iterations necessary may be large. But in later instances, the computation can commence with the former solution vector. If the atmospheric conditions have not changed very much meanwhile the old and new intensity distributions will be similar. Thus the number of necessary iterations can be greatly reduced. Therefore, the new method is fast enough to allow its implementation into mesoscale atmosphere models.

Appendix A

Properties of the Correction Function

Consider the situation of Figure 9 where 2×2 identical basic cells are joined together to form a square plate. We have to determine the transfer properties of this plate. The symmetry of the situation allows this problem to be reduced to the determination of one single intensity i, which flows from every cell to their two neighbours. All other intensities can be computed from this one, i. There are three contributions to i, namely the scattered unit test radiation, the reflected intensity i coming from one neighbour cell, and the scattered intensity i coming from the other neighbour. Thus:

$$i = S_0 + i\,(R_0 + S_0)\,, \;\Rightarrow\; i = S_0/\,(1 - R_0 - S_0)\,. \qquad (33)$$

The transmitted intensity consists of the directly transmitted radiation T_0 and of the scattered intensity i which comes from two directions:

$$T^*\,(2\tau_0) = T_0 + S_0 \cdot 2S_0/\,(1 - R_0 - S_0)\,. \qquad (34)$$

Therefore, $\mathscr{C}(2\tau_0) = 2\,S_0/(1 - R_0 - S_0)$, which is property (ii) of Section 5.2.

Next we proof that the correction function is strictly monotonically increasing with the number of basic cells in the plate. Let this number be $N \times N$. We write down the analytical solution for the radiative

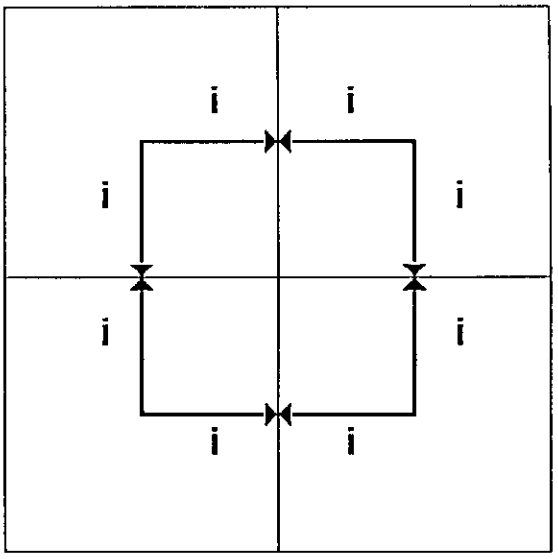

Figure 9 Square plate consisting of four identical basic cells. The direction of the unit test radiation is orthogonal to the paper plane. For the determination of the transfer properties of the plate it suffices to compute the intensity i, which flows from every cell into their two neighbours.

transfer problem through the plate, where the incident unit intensity flows into the – z direction:

$$\tilde{I}^{(\infty)} = (\mathbf{1} - \mathbf{Q})^{-1}\,\tilde{k}\,. \qquad (35)$$

$\mathbf{Q}$ describes the transport of photons within the plate. Since photons that flow in the $\pm z$ direction are lost from the plate, the corresponding columns in $\mathbf{Q}$ (every 5th and 6th) contain zeroes. The vector $\tilde{k}$ consists of N^2 times the subvector $(S_0, S_0, S_0, S_0, R_0, T_0)^\dagger$.

Let us now introduce a diagonal matrix $\mathbf{E}_6$ whose diagonal elements are zero except the 6th, 12th, ..., which are unity, i.e.

$$(\mathbf{E}_6)_{ij} = (\mathbf{1})_{ij}\,\delta\,(i \bmod 6)\,, \qquad (36)$$

where $\delta\,(\cdot)$ is the Kronecker symbol. The transmission probability for the plate can now be written in the form

$$T^*\,(N) = N^{-2}\,\|\mathbf{E}_6\,\tilde{I}^{(\infty)}\|_1\,. \qquad (37)$$

Thus we have to determine the 1-norm of $\mathbf{E}_6\,\tilde{I}^{(\infty)}$. Expanding $(\mathbf{1} - \mathbf{Q})^{-1}$ we get

$$\|\mathbf{E}_6\,\tilde{I}^{(\infty)}\|_1 = \|\mathbf{E}_6\,\tilde{k} + \mathbf{E}_6 \sum_{t=1}^{\infty} \mathbf{Q}^t\,\tilde{k}\,\|_1\,. \qquad (38)$$

The contribution of the first rhs term is $N^2 T_0$. The elements of $\tilde{k}$ that contribute to the second rhs term are all S_0 since in $\mathbf{Q}^t$ every 5th and 6th column vanishes. Therefore, $\|\mathbf{E}_6\,\Sigma_{t=1}^{\infty}\,\mathbf{Q}^t\,\tilde{k}\|_1 = S_0\,\|\mathbf{E}_6\,\Sigma_{t=1}^{\infty}\,\mathbf{Q}^t\|_1$.

Thus we can write

$$T^*(N) = T_0 + N^{-2} S_0 \| \mathbf{E}_6 \sum_{t=1}^{\infty} \mathbf{Q}^t \|_1 . \qquad (39)$$

If this is compared with the definition of the correction function we find the relation of $\mathscr{C}$ with the transfer operator $\mathbf{Q}$:

$$\mathscr{C}(N) = N^{-2} \| \mathbf{E}_6 \sum_{t=1}^{\infty} \mathbf{Q}^t \|_1 . \qquad (40)$$

Property (iii) of C is thus proven if we can show that $\| \mathbf{E}_6 \Sigma_{t=1}^{\infty} \mathbf{Q}^t \|_1$ grows stronger with N than N^2. It is

$$\| \mathbf{E}_6 \mathbf{Q}^t \|_1 = \sum_i \delta (i \bmod 6) \sum_j Q_{ij}^t . \qquad (41)$$

The sum over the column index j is the smallest for those values of i which correspond to a basic cell at the corner of the plate because a corner cell interacts with less neighbouring cells than all other cells. Let i_0 be such an index (with $i_0 \bmod 6 = 0$). Then a lower bound can be given for the above double sum if we replace Q_{ij} by $Q_{i_0 j}$ everywhere. This yields

$$\| \mathbf{E}_6 \mathbf{Q}^t \|_1 > N^2 \sum_j Q_{i_0 j}^t , \qquad (42)$$

which shows that all terms $\| \mathbf{E}_6 \mathbf{Q}^t \|_1$ are at least proportional to N^2. It remains to show that $\Sigma_{t=1}^{\infty} \Sigma_j Q_{i_0 j}^t$ grows with N.

Consider two plates with dimensions N^2 and $(N+1)^2$. For these, the partial sums $\Sigma_{t=1}^{N} \Sigma_j Q_{i_0 j}^t$ are equal since the corner cells in both plates have the same environment up to the N th generation of neighbour cells. However, for $t > N$ the interaction radius of the corner cell in the larger plate reaches additional cells, that do not exist in the smaller one. Thus, for all $t > N$ the terms in the above sum are larger for the larger plate, so that indeed $\Sigma_{t=1}^{\infty} \Sigma_j Q_{i_0 j}^t$ grows with N. This completes the proof.

Appendix B

The Factors α, β, and γ

Let the number of basic cells in a square plate be $N^2 = (\tau/\tau_0)^2$. Four of these are corner cells, 4 (N – 2) cells are located at the edge, and $(N-2)^2$ are inner cells.

For a photon that hits an arbitrary cell, the probability to be scattered into the plane of the plate equals the average number of immediate neighbours a cell has times S_0:

$$4\beta S_0 = \frac{4}{N^2} 2 S_0 + \frac{4(N-2)}{N^2} 3 S_0 + \frac{(N-2)^2}{N^2} 4 S_0 = 4 S_0 \left(1 - \frac{1}{N}\right). \qquad (43)$$

Hence, $\beta = 1 - \tau_0/\tau$.

A photon can change its direction within the plane either by 90° or by 180°. The 180° reversal is always possible. However, the cells are different with respect to the possible numbers of 90° scatterings that keep the photon within the plate. At the corners there is only one possibility, in the inner cells there are two. In an edge cell the photon has two possible scattering directions when it comes from an inner cell (with relative frequency 1/3), and one scattering direction when it comes from another cell at the edge (with relative frequency 2/3). The probability that the photon remains inside the plate in a scattering event is therefore:

$$2\gamma S_0 = \frac{4}{N^2} S_0 + \frac{4(N-2)}{N^2} \left(\frac{2}{3} S_0 + \frac{1}{3} 2 S_0\right) + \frac{(N-2)^2}{N^2} 2 S_0 = 2 S_0 \left(1 - \frac{4}{3N} + \frac{2}{3N^2}\right). \qquad (44)$$

This yields $\gamma = 1 - (4/3)(\tau_0/\tau) + (2/3)(\tau_0/\tau)^2$.

For the calculation of α we consider an arbitrary cell and count the number of cells that can be reached from this one in a series of transmissions. For each possible step we summarize the corresponding probability, i.e. $T_0^0 + T_0^1 + T_0^2 + \ldots$. We must regard all 4 directions and perform this procedure for all N^2 basic cells in the plate. α is then given by the total sum of the transmission probabilities divided by $4N^2$ (i.e. the number of directions times the number of basic cells). Thus we have

$$\alpha = (4N^2)^{-1} \sum_{i=1}^{N} \sum_{j=1}^{N} \left[\left(\sum_{k=0}^{M_i} + \sum_{k=0}^{m_i} + \sum_{k=0}^{M_j} + \sum_{k=0}^{m_j} \right) T_0^k \right], \qquad (45)$$

where $M_{i,j}$, $m_{i,j}$ are the number of cells from cell (i, j) to the edge in all 4 directions:

$$\begin{aligned} M_i &= \max(N-i-1, 0), \\ m_i &= \max(i-2, 0), \\ M_j &= \max(N-j-1, 0), \\ m_j &= \max(j-2, 0). \end{aligned} \tag{46}$$

For symmetry reasons it suffices to add the transmission probabilities for the cells in one quarter of the plate. The sums over k can be computed directly:

$$\begin{aligned} \alpha &= N^{-2} \sum_{i=1}^{N/2} \sum_{j=1}^{N/2} \frac{1}{1-T_0} (4 - T_0^{M_i+1} - \\ &\quad - T_0^{m_i+1} - T_0^{M_j+1} - T_0^{m_j+1}) \\ &= \frac{1}{1-T_0} \left[1 - T_0 N^{-2} \sum_{i=1}^{N/2} \sum_{j=1}^{N/2} (T_0^{M_i} + \right. \\ &\quad \left. + T_0^{m_i} + T_0^{M_j} + T_0^{m_j}) \right]. \end{aligned} \tag{47}$$

Since $N \geq 2$ and $i \leq N/2$, $M_i = N - i - 1$ (correspondingly for j). The double sum is symmetrical in the indices (i, j) and may thus be reduced to a simple sum over one index, where a factor N can be put out of the sum:

$$\alpha = \frac{1}{1-T_0} \left[1 - T_0 N^{-1} \sum_{i=1}^{N/2} (T_0^{N-i-1} + T_0^{m_i}) \right]. \tag{48}$$

Now we use $m_1 = 0$ and $m_i = i - 2$ for $i > 1$ and perform the summations. This yields after some simple algebra the desired result:

$$\alpha = \frac{1}{1-T_0} \left[1 - \frac{\tau_0}{\tau} \frac{2T_0 - T_0^2 - T_0^{(\tau/\tau_0)}}{1-T_0} \right]. \tag{49}$$

Acknowledgements

I thank Prof. Dr. U. Schumann, Dr. R. Sausen and Dr. D. Heimann for critically reading the manuscript, and Dr. S. Brinkop for many valuable discussions. I acknowledge the detailed opinion of the anonymous referee. The work was supported by the European Community (project EUCREX).

References

Bott, A., U. Sievers and *W. Zdunkowski,* 1990: A Radiation Fog Model with a Detailed Treatment of the Interaction between Radiative Transfer and Fog Microphysics. J. Atmos. Sci. **47**, 2153–2166.

Chu, C. M. and *S. W. Churchill,* 1955: Numerical Solution of Problems in Multiple Scattering of Electromagnetic Radiation. J. Chem. Phys. **59**, 855–863.

Cogley, A. C., 1981: Initial results for multidimensional radiative transfer by the adding/doubling method. Paper presented at the 4th Conference on Atmospheric Radiation, Am. Meteorol. Soc., Toronto, June 12–16.

Davies, R., 1978: The Effect of Finite Geometry on the Three-Dimensional Transfer of Solar Irradiance in Clouds. J. Atmos. Sci. **35**, 1712–1725.

Davis, A., P. Gabriel, S. Lovejoy, D. Schertzer and *G. L. Austin,* 1990: Discrete Angle Radiative Transfer, 3. Numerical Results and Meteorological Applications. J. Geophys. Res. **95**, 11729–11742.

Davis, J. M. and *S. K. Cox,* 1986: Additional Confirmation of the Validity of Laboratory Simulation of Cloud Radiances. J. Clim. Appl. Meteor. **25**, 398–400.

Deirmendjian, D., 1969: Electromagnetic Scattering on Spherical Polydispersions. Elsevier, New York, 290 pp.

Gabriel, P., S. Lovejoy, A. Davis, D. Schertzer and *G. L. Austin,* 1990: Discrete Angle Radiative Transfer, 2. Renormalization Approach for Homogeneous and Fractal Clouds. J. Geophys. Res. **95**, 11717–11728.

Goodman, R., 1988: Introduction to Stochastic Models. Benjamin/Cummings, Menlo Park (Ca), 368 pp.

Gube, M., J. Schmetz and *E. Raschke,* 1980: Solar radiative transfer in a cloud field. Beitr. Phys. Atmosph. **53**, 24–34.

Liou, K. N. and *Q. Zheng,* 1984: A Numerical Experiment of the Interactions of Radiation, Clouds and Dynamic Processes. J. Atmos. Sci. **41**, 1513–1535.

Lovejoy, S., A. Davis, P. Gabriel, D. Schertzer and *G. L. Austin,* 1990: Discrete Angle Radiative Transfer, 1. Scaling and Similarity, Universality and Diffusion. J. Geophys. Res. **95**, 11699–11715.

Preisendorfer, R. W., 1965: Radiative Transfer On Discrete Spaces. Pergamon Press, Oxford, 462 pp.

Rockel, B., E. Raschke and *B. Weyres,* 1991: A Parameterization of Broad Band Radiative Transfer Properties of Water, Ice, and Mixed Clouds. Beitr. Phys. Atmosph. **64**, 1–12.

Starr, D. O'C. and *S. K. Cox,* 1985: Cirrus Clouds, Part I: A Cirrus Cloud Model. J. Atmos. Sci. **42**, 2663–2681.

Somieski, F., P. Koepke, K. T. Kriebel and *R. Meerkötter,* 1988: Improvements of Simple Radiation Schemes for Mesoscale Models: a Case Study. Beitr. Phys. Atmosph. **61**, 204–218.

Trautmann, T. and *W. Zdunkowski,* 1986: Transfer of solar radiation in a regular field of rectangular clouds. Meteorol. Rdsch. **39**, 66–74.

Varga, R. S., 1962: Matrix Iterative Analysis. Prentice-Hall, Englewood Cliffs (N.J.), 322 pp.

Welch, R. M. and *W. G. Zdunkowski,* 1981: The Radiative Characteristics of Noninteracting Cumulus Cloud Fields, Part I: Parameterization for Finite Clouds. Beitr. Phys. Atmosph. **54**, 258–272.